PAPER

Near-infrared to violet triplet−triplet annihilation fluorescence upconversion of Os(ii) complexes by strong spin-forbidden transition†

Yaxiong Wei,[a] Min Zheng,[a] Lin Chen,*[b] Xiaoguo Zhou ID *[a] and Shilin Liu ID [a]

Three Os(ii) complexes were synthesized with ligands 2,2'-dipyridyl (dipy), 1,10-phenanthroline mono-hydrate (phen), and 4,7-diphenyl-1,10-phenanthroline (diphen), and applied as triplet photosensitizers for triplet−triplet annihilation (TTA) fluorescence upconversion. The strong spin-orbital coupling made direct spin-forbidden transition of $S_0−T_1$ feasible. Lifetimes of the lowest triplet state of these complexes were determined to be 107 ns, 373 ns, and 386 ns for Os-dipy, Os-phen, and Os-diphen, respectively, using nanosecond transient absorption spectra. From steady-state phosphorescence emission spectra, energies of the triplet states were derived to be 1.75 eV, 1.80 eV, and 1.74 eV for Os-dipy, Os-phen, and Os-diphen, respectively. Using these photosensitizers, strong upconverted fluorescence of the triplet acceptors, 9,10-diphenylanthracene (DPA), perylene, and 9,10-bis(phenethynyl) anthracene (BPEA), was observed in the visible to violet range. In particular, fluorescence emission with the largest anti-Stokes shift of 1.14 eV was observed for the Os-phen/DPA system, and the upconverted quantum yield was determined as 5.9% in deoxygenated dichloroethane. Additionally, upconversion was determined in air using mixtures of dichloroethane and DMSO solvents, and the maximal quantum yield was measured to be 4.5% for Os-phen/DPA.

Introduction

Photon upconversion is a process in which the material produces higher energy photons on irradiation with lower energy photons.[1] Among the various well-known upconversion approaches, triplet–triplet annihilation (TTA) upconversion fluorescence is especially promising because of its low power density requirement (only a few mW cm^{-2}, less than the solar power density of ~100 mW cm^{-2} at AM 1.5) and a relatively high efficiency under weak irradiation intensity.[2–4] In the past decades, TTA upconversion has been applied in numerous fields, including photovoltaics,[5,6] photoelectrochemistry,[7] photocatalysis,[8,9] and fluorescent cell imaging.[10,11]

[a]Hefei National Laboratory for Physical Sciences at the Microscale, iChEM (Collaborative Innovation Center of Chemistry for Energy Materials), Department of Chemical Physics, University of Science and Technology of China, Hefei, Anhui 230026, China. E-mail: xzhou@ustc.edu.cn
[b]School of Physics and Materials Engineering, Hefei Normal University, Hefei, Anhui 230601, China. E-mail: chenlin@hfnu.edu.cn
† Electronic supplementary information (ESI) available: Experimental apparatus and measurement procedures; NMR spectra; transient absorption spectra and dynamic decay curves; TTA upconversion spectra; absorption and fluorescence spectra of Os(ii) complexes; detailed DFT calculation results. See DOI: 10.1039/c9dt02276g

For light harvesting in a TTA upconversion system, a large number of triplet photosensitizers have been synthesized.[12–16] The photosensitizers based on transition metals or heavy atoms such as Ir(ii), Pt(ii), Ru(ii), I, and Br, are particularly popular because of efficient intersystem crossing (ISC) induced by strong spin–orbit coupling.[3,7,17,18] Several organic compounds, *e.g.*, 2,3-butanedione and benzophenone, also exhibit efficient ISC because of a small energy gap between the S_1 and T_1 states in low-lying n–π* transitions.[19] Yet another type of photosensitizers are the fullerene family, *i.e.*, C_{60} and C_{70}, since they are common intramolecular spin converters with ISC efficiency of unity.[20–24] Recently, radical-enhanced ISC and spin–orbit charge transfer have been used to design a novel triplet photosensitizer.[25] However, taking into account the energy loss from S_1–T_1, the anti-Stokes shift of upconverted fluorescence has usually been reduced to less than 0.8 eV.[13]

The anti-Stokes shift is one of the most important parameters of a TTA upconversion system for solar energy application. To utilize solar light efficiently, a large anti-Stokes shift of upconverted fluorescence is necessary. A creative strategy to increase the anti-Stokes shift involves minimizing the energy loss of ISC in the formation of triplet photosensitizers, such as thermally activated delayed fluorescence (TADF),[26,27] or direct singlet-to-triplet (S–T) excitation.[28–30] Generally, TADF molecules have a small S_1–T_1 gap, but the related absorption is

always located in the blue and violet spectral regions.[31,32] Compared to the TADF method, direct S–T excitation is more practical because the absorptions are located in the near-infrared region.[33,34] However, the direct S–T excitation is spin-forbidden for most compounds, so that the molar absorption coefficients are extremely small (<10 M^{-1} cm^{-1}).[28] In 2005, Altobello *et al.*[33] reported a terpyridyl Os(II) complex as the first successful photosensitizer of direct S–T excitation. The S–T absorption at 1100 nm was accompanied with metal-to-ligand charge transfer (MLCT). Recently, Amemori *et al.*[30] applied other Os(II) complexes as triplet photosensitizers in the TTA upconversion of Rubrene, and the anti-Stokes shift was promoted up to 0.86 eV with quantum yield (Φ_{UC}) of 3.1% in solid films. However, the triplet–triplet energy transfer (TTET) efficiency and the quantum yield were found to be significantly low in solutions as the triplet lifetime was only 12 ns. The same authors have also reported a new triplet photosensitizer, Os(bptpy)$_2^{2+}$, for direct S–T absorption later.[29] According to the extended triplet lifetime (207 ns), the anti-Stokes shift was further increased to 0.97 eV, and the Φ_{UC} was 2.7% in *N,N*-di-methylformamide (DMF) solutions. Very recently, Liu *et al.*[28] synthesized an Os(II)-tris(bpy) complex by attaching a Bodipy moiety. The triplet state lifetime was markedly extended to 1.73 μs. The Φ_{UC} value was measured to be 1.2% with *N,N'*-bis(3-pentyl)perylene-3,4,9,10-bis(dicarboximide) (PBI) as an energy acceptor, however, the anti-Stokes shift was only 0.3 eV. In the TTA upconversion mechanism, the TTET process is usually rate-determining.[35] Thus, a brief lifetime of the triplet photosensitizer prepared by direct S–T transition significantly diminishes TTET efficiency[29,30] and leads to unsatisfying performances. Moreover, the relatively large energy gaps between the triplet states of photosensitizers and acceptors cause extra energy loss in the TTET process.[28,29]

Using different ligands, the lowest triplet energies of the complexes can be altered purposefully.[36] Thus, we synthesized three Os(II) complexes, namely, Os-dipy, Os-phen, and Os-diphen, with 2,2′-dipyridyl (dipy), 1,10-phenanthroline monohydrate (phen), and 4,7-diphenyl-1,10-phenanthroline (diphen), respectively, to prolong the lifetimes of triplet photosensitizers and find consistent partners of TTET to reduce the extra energy loss. Among the three photosensitizers, Os-dipy was reported, however its performance in TTA upconversion application was unsatisfied (the anti-Stokes shift was 0.3 eV and Φ_{UC} was 1.2%).[28] Scheme 1 shows the molecular structures of these triplet photosensitizers and acceptors. Using steady-state and transient absorption/emission spectroscopy, the photophysical properties of these Os(II) complexes, such as lifetimes and excitation energies of the triplet states, were investigated. Based on the triplet energies of the complexes, DPA, perylene, and BPEA were chosen as triplet acceptors. According to the direct S–T excitation and the matched triplet energies, a larger anti-Stokes shift (1.14 eV) than the reported values was achieved in the TTA upconversion system involving Os(II)-phen and DPA in solutions. Moreover, the mixed solvent of DMSO and dichloroethane was tested for these upconversion systems, to find a simple and feasible way to apply them in air.
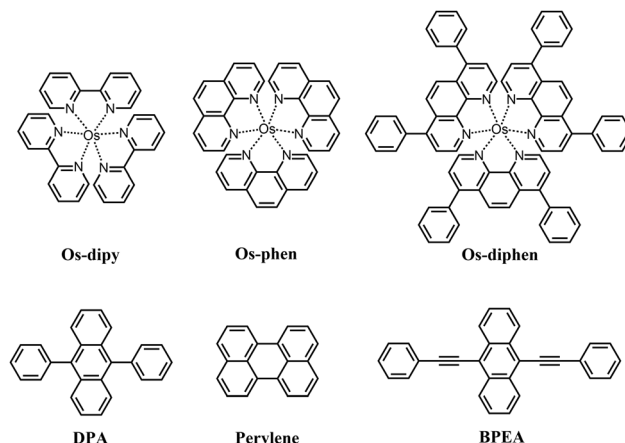

Scheme 1 Molecular structures of the photosensitizers, Os-dipy, Os-phen, Os-diphen, and the energy acceptors, 9,10-Diphenylanthracene (DPA), perylene, and 9,10-bis(2-phenylethynyl)-anthracene (BPEA).

Results and discussion

Steady-state UV-Vis absorption and phosphorescence spectra

The UV-Vis absorption spectra of the photosensitizers in dichloroethane are shown in Fig. 1a. The Os(II) complexes exhibited similar spectral absorptions, involving a doublet absorption in the region of 400–550 nm and a weak peak at ~660 nm with a long-wavelength tail. For Os-phen in dichloroethane, two intense singlet–singlet absorption peaks were observed at 432 nm ($\varepsilon = 29\,000$ M^{-1} cm^{-1}) and 480 nm ($\varepsilon = 26\,000$ M^{-1} cm^{-1}), both of which were assigned as the singlet–singlet MLCT transitions. In contrast, the weak and broad absorption of singlet–triplet MLCT transition was also identified, although dim double peaks were observed. For Os-diphen, the double singlet–singlet absorptions were located at 450 nm ($\varepsilon = 41\,000$ M^{-1} cm^{-1}) and 501 nm ($\varepsilon = 35\,000$ M^{-1} cm^{-1}), while the singlet–triplet transition peak covered a range of 560–720 nm with a molar absorption coefficient of 7300 M^{-1} cm^{-1} at 682 nm. For Os-dipy, more absorption peaks were observed in the wavelength region. The singlet–singlet absorptions were observed at 370 nm ($\varepsilon = 14\,000$ M^{-1} cm^{-1}), 436 nm ($\varepsilon = 17\,000$ M^{-1} cm^{-1}), and 483 nm ($\varepsilon = 17\,000$ M^{-1} cm^{-1}), while the singlet–triplet band was located at
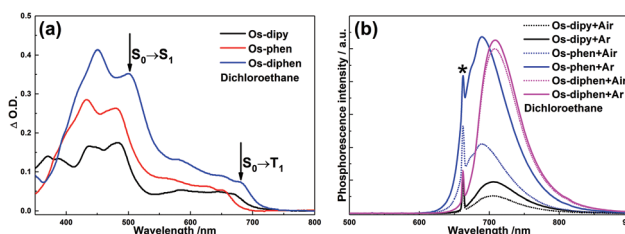
Fig. 1 (a) Steady-state UV-Vis absorption spectra of Os-dipy, Os-phen, and Os-diphen. (b) Phosphorescence emission spectra ($\lambda_{ex} = 663$ nm) of Os-dipy, Os-phen, and Os-diphen. Dichloroethane as solvent, $c = 1 \times 10^{-5}$ M, 25 °C.

667 nm (ε = 4400 M^{-1} cm^{-1}). Moreover, the concentration-dependencies of absorption spectra of the Os(II) complexes were studied (see ESI, Fig. S1–S4†). The absorption intensity changed linearly with the concentration of the complexes, indicating that no aggregation of the complexes occurred in solution within the experimental concentration range.

The fluorescence emission spectra of the complexes were measured (see ESI, Fig. S5†) under photoexcitation at 450 nm (singlet–singlet absorption). The fluorescence emission from the singlet electronically excited state was very weak in the region of 500–550 nm, implying a high ISC efficiency. In contrast to fluorescence, the phosphorescence emissions of these complexes were very evident. Fig. 1b shows the phosphorescence spectra of the complexes in dichloroethane under photoexcitation at 663 nm (direct S–T transition). For Os-dipy, the emission covered a broad region of 600–900 nm with a peak at 707 nm, and thus the excitation energy of the triplet state was determined as 1.75 eV. Owing to quenching by oxygen molecules, the phosphorescence from the triplet state was weak in air, but more than doubled under argon. The phosphorescence quantum yield was determined as 0.4% in air and 0.9% in argon. For Os-phen in dichloroethane, the emission peak was located at 690 nm, and hence the excitation energy of the triplet state was 1.80 eV. Compared to Os-dipy, Os-phen showed stronger phosphorescence emission, and the quantum yield was increased to 2.0% in air and 5.5% in argon. When two phenyls were attached to 1,10-phenanthroline, the extent of conjugation in the Os(II) complex was further enhanced in Os-diphen. As a result, the excitation energy of the triplet state was lowered to 1.74 eV, since the phosphorescence emission peak was red-shifted to 711 nm. However, the quantum yield was almost unchanged. Table 1 summarizes the photophysical properties of the three Os(II) complexes in dichloroethane.

Transient absorption spectra and quenching rate constant

In the presence of triplet acceptors, TTET can occur once the triplet state of the photosensitizer is prepared. Nanosecond transient absorption spectra and kinetic curves of the characteristic absorptions were performed for Os-dipy, Os-phen, and Os-diphen. Since ISC of these photosensitizers were very

Table 1 Photophysical properties of the Os(II) complexes in dichloroethane[a]

Compound	λ_{abs}[b]	ε (s)[c]	λ_{abs}[b]	ε (t)[c]	λ_{em}[b]	Φ_P (air)[d]	Φ_P (Ar)[d]
Os-dipy	370/436/483	1.4/1.7/1.7	667	0.44	707	0.4	0.9
Os-phen	432/480	2.9/2.6	654	0.53	690	2.0	5.5
Os-diphen	450/501	4.1/3.5	682	0.73	711	2.2	4.4

[a] c[Complex] = 1.0×10^{-5} M. [b] Peak positions of absorption and emission spectra, in unit of nm. [c] Molar extinction coefficient at maximal absorption, 's' is singlet excitation, 't' is triplet excitation, in 10^4 M^{-1} cm^{-1}. [d] Phosphorescence quantum yield, using methylene blue as a standard (Φ_{FL} = 3%).

Table 2 bimolecular quenching rate constants (in 10^9 M^{-1} s^{-1}) of different acceptors[a]

Compounds		Os-dipy	Os-phen	Os-diphen
–	τ_0	107	373	386
DPA	τ	70	67	208
	Φ_{TTET}	0.35	0.82	0.46
	k_q	0.39	0.82	0.16
perylene	τ	45	56	93
	Φ_{TTET}	0.58	0.85	0.76
	k_q	3.01	2.99	1.89
BPEA	τ	69	112	198
	Φ_{TTET}	0.36	0.7	0.49
	k_q	1.89	1.79	0.96

[a] c[Photosensitizer] = 1×10^{-5} M, c[DPA] = 1.5×10^{-2} M, c[Pery] = 5×10^{-3} M, c[BPEA] = 3.3×10^{-3} M.

efficiency, their following kinetic behaviours had no difference after photoexcitation along singlet–singlet or singlet–triplet transitions. Thus, for convenience, the nanosecond time-resolved measurements were performed at excitation at 532 nm. The lifetimes of the triplet state, τ_0, TTET efficiencies from photosensitizers to acceptors, Φ_{TTET}, and the bimolecular quenching rate constants, k_q, were obtained and listed in Table 2.

Since the three complexes showed similar spectra and kinetic behaviors, only the transient absorption spectra and kinetic curves of Os-phen have been shown in Fig. 2a and b as an example. For Os-phen in dichloroethane, a very strong phosphorescence emission at 728 nm was observed together with two weak ground-state bleaching (GSB) peaks at 444 nm and 494 nm. Owing to its extremely weak intensity, the triplet excited state absorption (ESA) could not be clearly observed in the range of 400–850 nm. Thus, the lifetime of the triplet state of Os-phen was derived from the decay rate of phosphorescence emission as 373 ns (Fig. 2b). For Os-dipy, the phosphorescence emission of the triplet state was observed at 725 nm, accompanied with a weak GSB at 450 nm (see ESI, Fig. S6†). The lifetime of the triplet Os-dipy was as short as 107 ns (see ESI, Fig. S7†), which was consistent with the previous data.[28] For Os-diphen, the photophysical features of the triplet state were very similar to those of Os-phen. Two GSB bands were observed at 460 nm and 510 nm, in addition to a phosphorescence emission at 727 nm, and the triplet state lifetime was determined as 386 ns (see ESI, Fig. S8 and S9†).

In the presence of triplet acceptors, TTET from the triplet photosensitizers is feasible. Considering the T_1 energies of the photosensitizers in dichloroethane, DPA (T_1 = 1.77 eV), perylene (T_1 = 1.53 eV), and BPEA (T_1 = 1.25 eV) were chosen as the triplet acceptors in this study. As shown in Fig. 2b, the triplet lifetime of Os-phen was reduced in the presence of the acceptors. Through fitting the decay curve of the absorption at 720 nm at different concentrations of the acceptors, the apparent lifetime of the triplet complex, τ, was obtained. Using the
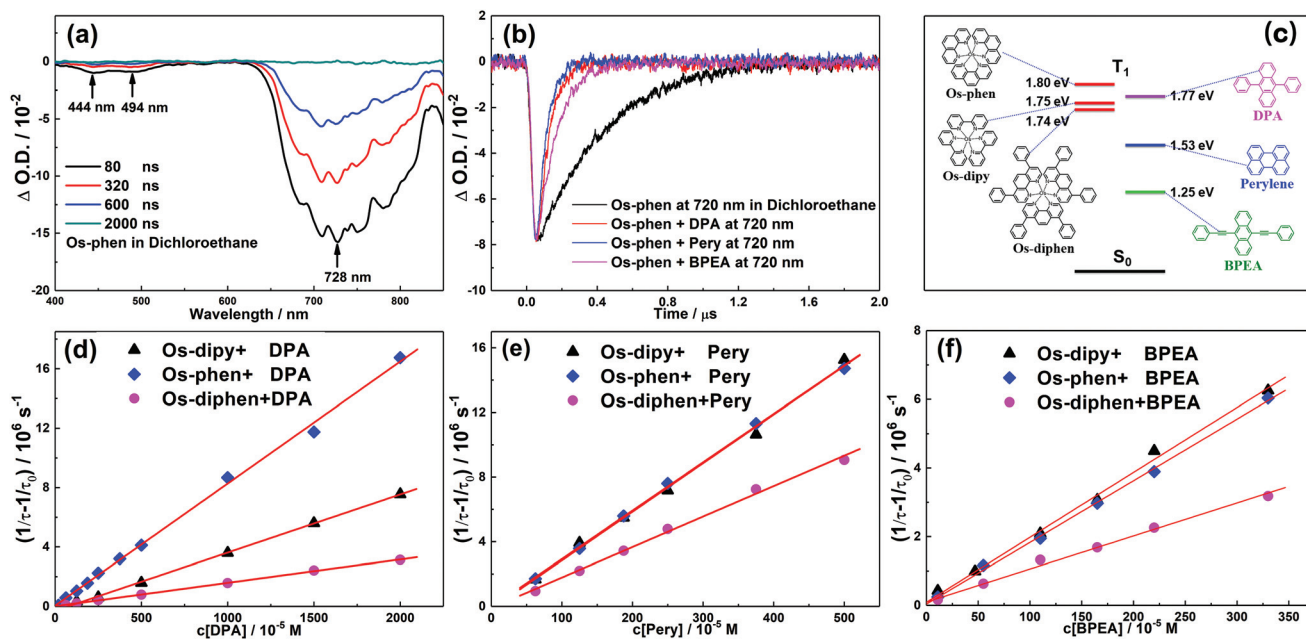
Fig. 2 (a) Nanosecond transient absorption spectra of Os-phen. (b) Decay curve of Os-phen at 720 nm in the presence of different acceptors. (c) Energy diagram of the lowest triplet states of photosensitizers and acceptors. (d–f) Bimolecular quenching rates of the triplet photosensitizers by different concentrations of the acceptors. c[Photosensitizer] = 1×10^{-5} M, in dichloroethane, λ_{ex} = 532 nm, 25 °C.

Stern–Volmer eqn (1), bimolecular quenching rate constant, k_q, was determined (Fig. 2d–f), and TTET efficiency, Φ_{TTET}, was calculated using eqn (2).

$$1/\tau - 1/\tau_0 = k_q \, [\text{acceptor}] \qquad (1)$$

$$\begin{aligned}
\Phi_{TTET} &= (k_{TTET} \cdot [\text{acceptor}])/(k_{TTET} \cdot [\text{acceptor}] + k_{NR}) \\
&= (1/\tau - 1/\tau_0)/(1/\tau)
\end{aligned} \qquad (2)$$

where τ_0 and τ are the triplet lifetimes of the Os(II) complexes in the absence and presence of acceptors, respectively. The k_q and Φ_{TTET} values of the photosensitizers quenched by different acceptors are summarized in Table 2. For DPA, k_q showed a remarkable dependence on the type of the photosensitizer, e.g., 0.39×10^9 M^{-1} s^{-1} for Os-dipy, 0.82×10^9 M^{-1} s^{-1} for Os-phen, and 0.16×10^9 M^{-1} s^{-1} for Os-diphen, although the molecular structures of the complexes were not dissimilar. In the case of Os-dipy and Os-diphen, similar results were observed with the three acceptors (see ESI, Fig. S7 and S9†).

In principle, the apparent TTET rate between the photosensitizer and acceptor in solutions is determined by the formation rate of contact pair by diffusion and the TTET efficiency in a solvent cage. The former can be calculated as the diffusion rate, while the latter generally depends on the energy gap between the triplet photosensitizer and acceptor. A small energy loss from the triplet photosensitizer to the acceptor implies higher TTET efficiency. In the present experiments, the diffusion rate, $k_{diffuse}$, was theoretically determined as $8k_B T/3\eta = 8.1 \times 10^9$ M^{-1} s^{-1} (where η is the viscosity of dichloroethane, 0.84 mPa s at 25 °C). It is evident that all the k_q values

of the complexes were much lower than $k_{diffuse}$. Thus, TTET in a solvent cage is the rate-determining step.

As shown in Fig. 2c, the triplet energies of Os-phen and DPA were most proximate, and therefore, they were the best energy partners. The slightly higher energy of triplet Os-phen (1.80 eV) than that of DPA (1.77 eV) facilitated the TTET process. The triplet energies of Os-dipy and Os-diphen were slightly lower, i.e., 1.75 eV and 1.74 eV, respectively. However, the mean thermal activated energy at room temperature (25 °C) was estimated as RT = 0.026 V, and thus, TTETs from these two Os(II) complexes to DPA were still feasible, albeit with slower rates. When perylene and BPEA were used as acceptors, all the Os(II) complexes had enough active energy to perform TTET to form triplet acceptors, but the energy loss was larger (e.g., 0.25 eV from Os-phen to perylene, 0.55 eV from Os-phen to BPEA, 0.49 eV from Os-diphen to BPEA). In summary, all the k_q values agreed with the theoretical deductions based on the TTET process.

DFT calculations on the frontier molecular orbitals

To gain further insight into the photophysical features of the Os(II) complexes, DFT calculations of their frontier molecular orbitals were performed.[37] The excitation energies, oscillator strengths, and main configurations of the low-lying electronic excited states of the Os(II) complexes are summarized in Tables S1–S3 of ESI.† For instance, in the case of Os-phen, the dominant configurations of the UV-Vis absorptions and the energy gap between the lowest triplet state and ground state can be seen in Fig. 3a. All the major absorptions in the UV-Vis range were accompanied with MLCT. The other two complexes displayed similar characteristics (see ESI, Fig. S10 and S11†).
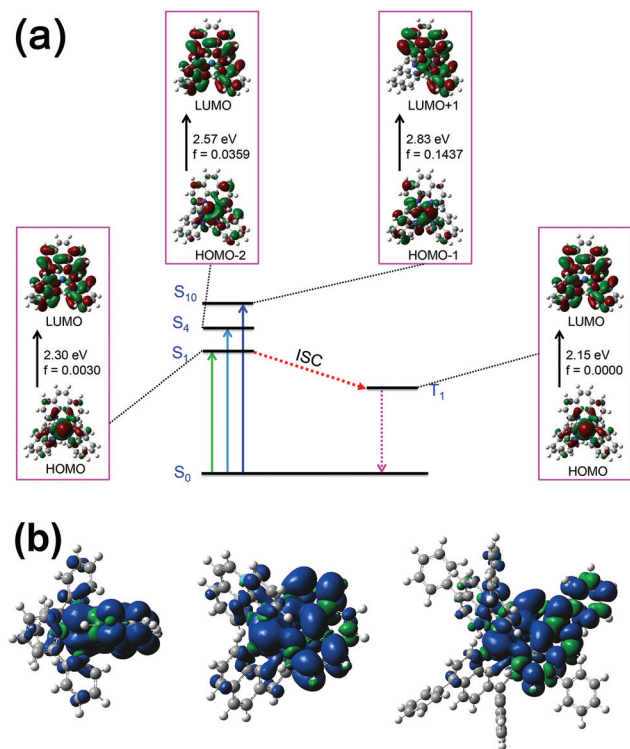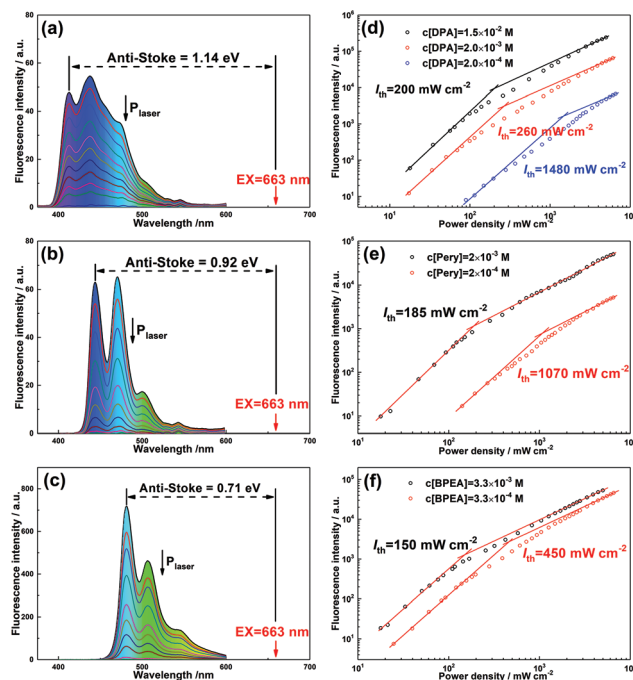
Fig. 3 (a) Frontier molecular orbitals involved in the low-lying singlet and triplet excited states of the photosensitizers. (b) Spin density surfaces obtained by optimizing the triplet excited states. Calculations were performed at the B3LYP/6-31G(d) level. Acetonitrile was used as the solvent.

Fig. 4 (a–c) Upconverted fluorescence emission spectra under different excitation power densities, where Os-phen was the photosensitizer, and DPA (2.0×10^{-4} M), perylene (2.0×10^{-4} M), and BPEA (3.3×10^{-4} M) were the acceptors. (d–f) Double logarithmic plot of the upconverted fluorescence intensity as a function of excitation power density. Dichloroethane as the solvent, c[photosensitizer] = 1×10^{-5} M, λ_{ex} = 663 nm, 25 °C.

According to the DFT calculations, the energy differences of HOMO–LUMO were determined to be 2.24 eV for Os-dipy, 2.30 eV for Os-phen, and 2.23 eV for Os-diphen, which shows the same trend as the Redox potential results (see ESI Table S4†). However, the UV-visible absorption spectra are greatly broadened mainly owing to the thermal distribution of molecular vibration, leading to that the HOMO–LUMO energy intervals derived from the absorption spectra have relatively large uncertainty (see ESI Table S4†). Fig. 3b shows the spin density surfaces of the lowest triplet states of the complexes. In the triplet states, the spin densities were mainly distributed on the Os(II) atom and one ligand. Thus, TTET was inevitably restricted by steric hindrance in a solvent cage, leading to a lower k_q value than $k_{diffuse}$. Particularly, for Os-diphen, ligand inhibition was more obvious, resulting in the lowest k_q value among the three complexes (Table 2).

TTA upconversion fluorescence spectra in deoxygenated dichloroethane

The upconverted fluorescence spectra of the triplet acceptors when they were photoexcited at 663 nm in deoxygenated Os-phen/dichloroethane solution are shown in Fig. 4a–c.† When DPA was used as the acceptor, blue and violet emission was clearly observed and exhibited an anti-Stokes shift of 1.14 eV. For photosensitizers Os-dipy and Os-diphen, similar fluo-

rescence spectra were obtained in deoxygenated dichloroethane, as shown in Fig. S12–S14 of ESI.†

In the present TTA upconversion system, four kinetic subprocesses are involved, such as spin-forbidden absorption, TTET to triplet acceptors, TTA, and fluorescence emission of the acceptors. Thus, to achieve higher TTA upconversion quantum yield, a high concentration of the acceptor is usually recommended to saturate the TTET process. However, the self-absorption of the acceptor at too high concentrations may reduce the fluorescence quantum yield. In comparison with the fluorescence spectrum of DPA itself (Fig. 5d), the band intensity at 417 nm in the upconverted fluorescence spectrum of Fig. 4a was reduced in some extent relative to the other nearby peaks, confirming the self-absorption effect. Thus, it was necessary to assess the effect of acceptor concentration on Φ_{UC} in the experiments.

Fig. 5a–c show the dependence of the upconverted fluorescence intensity on the acceptor concentration. For Os-dipy and Os-diphen, the upconverted fluorescence intensity of DPA was linearly enhanced with its concentration, implying that the TTET stage was rate-determining in the overall TTA upconversion process. For Os-phen, the fluorescence intensity was quickly increased and then gradually became saturated at ~1.0 × 10^{-2} M. A similar phenomenon was observed for BPEA as the acceptor, although the saturation concentration was slightly reduced. However, perylene showed a different relationship
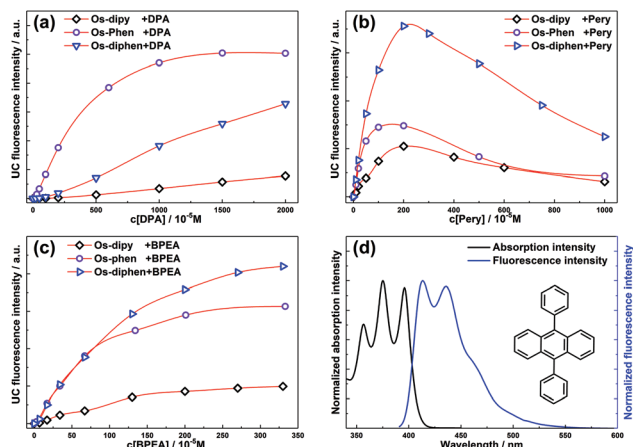
Fig. 5 Effect of concentration of (a) DPA, (b) perylene, and (c) BPEA on TTA upconversion fluorescence intensity, together with the UV-Vis absorption and fluorescence emission spectra of DPA itself (d). c[Photosensitizer] = 1 × 10^{-5} M, dichloroethane as solvent, λ_{ex} = 663 nm, with a power density of 3800 mW cm^{-2}, 25 °C.

Table 3 Φ_{UC} of the present TTA upconversion systems[a]

Compound	Φ_{UC} (dichloroethane, Ar, %)[b]			Φ_{UC} (DMSO, Air, %)[c]		
	DPA	Perylene	BPEA	DPA	Perylene	BPEA
Os-dipy	0.4	1.1	3.0	—[d]	0.05	0.03
Os-phen	5.9	2.3	12.5	0.11	0.32	0.22
Os-diphen	1.2	2.5	10.3	<0.01	0.38	0.25

[a] c[Photosensitizer] = 1.0 × 10^{-5} M. [b] Φ_{UC} in deoxygenated dichloroethane, where c[DPA] = 1.5 × 10^{-2} M, c[perylene] = 2.0 × 10^{-3} M, and c[BPEA] = 3.3 × 10^{-3} M. [c] Φ_{UC} in aerated DMSO, where c[DPA] = 5.0 × 10^{-3} M, c[perylene] = 5.0 × 10^{-3} M, and c[BPEA] = 6.7 × 10^{-4} M. [d] Upconverted fluorescence was unobserved.

(Fig. 5b), where the maximal fluorescence intensity was obtained at 2.0 × 10^{-3} M concentration and then decreased with increasing concentration. It is suggested that the self-absorption would be considerable for perylene at high concentration. In the present experiments, the optimized acceptor concentrations of DPA, perylene, and BPEA were determined as 1.5 × 10^{-2} M, 2.0 × 10^{-3} M, and 3.3 × 10^{-3} M in deoxygenated dichloroethane, and 5.0 × 10^{-3} M, 5.0 × 10^{-3} M, and 6.7 × 10^{-4} M in DMSO, respectively.

It is well known that the upconverted fluorescence intensity has a quadratic dependence on the excitation power at low intensities and transforms to a linear dependence at higher power densities. Thus, an important parameter, I_{th}, is defined as the threshold excitation power density of TTA upconversion. When the power density is lower than I_{th}, Φ_{UC} is linearly dependent on the incident laser power. Once the power density becomes greater than I_{th}, Φ_{UC} reaches its maximum, and the TTA process becomes the dominant deactivation pathway for the triplet acceptors. Therefore, the Φ_{UC} values at the power density beyond I_{th} are usually used to evaluate the quality of the photosensitizer.

As shown in Fig. 4d, the I_{th} value was determined as 1480 mW cm^{-2} for Os-phen with the DPA concentration of 2.0 × 10^{-4} M. When the DPA concentration was increased to 1.5 × 10^{-2} M, I_{th} was reduced to 200 mW cm^{-2}. This relationship agreed with the fact that the TTET efficiency was reduced with a decrease in the acceptor concentration. According to previous study,[38] the I_{th} was proportional to the reciprocal of TTET efficiency Φ_{TTET}. In the present experiments, the linear relationship between I_{th} and $1/\Phi_{TTET}$ was observed (ESI Fig. S15†). For perylene and BPEA as acceptors, similar dependencies of fluorescence intensity on power density were observed (Fig. 4e and f). The I_{th} value was determined as 185 mW cm^{-2} for perylene (2.0 × 10^{-3} M) and 150 mW cm^{-2} for BPEA (3.3 × 10^{-3} M).

Table 3 lists the measured Φ_{UC} values at the power density beyond I_{th}. Although Os-diphen had the most intense absorption ability in the region, its inefficient TTET led to the slightly poorer behavior. Os-dipy showed the worst Φ_{UC} value due to its shortest triplet lifetime (Table 2). Os-phen showed the best performance among the three complexes, e.g. Φ_{UC} = 5.9%, 2.3%, and 12.5% for DPA, perylene, and BPEA in dichloroethane, respectively. It is worth noting that in the TTA upconversion system of Os-phen/DPA, the anti-Stokes shift was up to 1.14 eV. This is the largest reported value of all reported solution upconversion systems,[13,27,29,39,40] and its I_{th} value is even lower than those of similar systems.[29,30] The observations strongly suggest that Os-phen/DPA in deoxygenated dichloroethane is a suitable candidate for TTA upconversion in solar energy applications.

TTA upconversion fluorescence spectra in aerated solutions

Because oxygen molecules can quickly quench triplet photosensitizers, the majority of TTA upconversion systems have been established in deoxygenated solutions. This shortcoming significantly restricts their practical application. In order to eliminate the effect of oxygen molecules, several interesting methods have been developed, such as addition of oxygen scavengers in solutions,[41,42] using solutions with low dissolved oxygen-like oils,[43] or applying polyphosphates as a protective matrix.[44] However, adding such substances may affect the absorption of the photosensitizer and fluorescence emission of the acceptor owing to change in solvent polarity, making the overall kinetics more complicated and reducing the Φ_{UC} value.

Recently, a long-lived phosphorescence emission of Au complexes was observed in aerated DMSO solution,[45] suggesting that DMSO is a solvent with low solubility of oxygen and especially suitable for TTA upconversion without deoxygenation. It was confirmed later that DMSO reacts with singlet oxygen to produce methyl sulfone.[46] Therefore, both sulfoxides and cyclic ureas were deemed to be photochemically deoxygenating solvents.[46] Herein, the present TTA upconversion systems of Os(II) complexes were tested in aerated DMSO solutions to compare with those in deoxygenated dichloroethane.

The Φ_{UC} values measured in aerated DMSO solutions are listed in Table 3. Compared to those in deoxygenated dichloroethane, the Φ_{UC} values were much lower in aerated DMSO, e.g.,

0.11% for Os-phen/DPA. No upconverted fluorescence was observed in the case of Os-dipy/DPA. These results are unsurprising, because the fluorescence quantum yields of the acceptors in DMSO were clearly reduced as a result of the increase of polarity.[18] Moreover, the viscosity of DMSO, η_{DMSO}, is as large as 1.996 mPa s, so that the formation rate of encounter by collision is reduced, and confines the TTET process remarkably.[18]

To obtain higher Φ_{UC} in aerated solutions, a simple strategy is to use mixed solvents of DMSO and dichloroethane, since these have reduced viscosities ($\eta_{dichloroethane}$ = 0.84 mPa s) and can improve the fluorescence quantum yield of an acceptor. Furthermore, the advantageous attribute of DMSO of consuming singlet oxygen can be retained as well. Fig. 6a–c show the TTA upconversion fluorescence spectra of Os-phen/acceptors systems in mixed solvents with different molar fractions of DMSO. The dependence of the upconverted fluorescence intensity on the DMSO molar fraction is plotted in Fig. 6d.

Although the phosphorescence spectra of the photosensitizers were visibly changed with the varying DMSO fraction, TTA upconversion spectra were not significantly affected except for their intensity (Fig. 6a–c). Interestingly, the upconverted fluorescence intensities of different acceptors exhibited different dependencies on the DMSO fraction. When perylene and BPEA were used as triplet acceptors, the upconverted fluorescence was enhanced with the increasing DMSO fraction and reached the maximum at 30% (Fig. 6d), where Φ_{UC} was enhanced nearly three-fold for perylene (0.8%) and BPEA (0.7%). However, when the DMSO fraction was increased beyond 30%, the upconverted fluorescence intensity was gradually reduced. According to approximate dissolved oxygen levels of DMSO and dichloroethane, the oxygen concentration itself in solutions was not significantly changed with the DMSO fraction. In

principle, the reaction between DMSO and singlet oxygen can quickly consume the dissolved oxygen, reducing the quenching of the triplet acceptors by oxygen, thereby enhancing fluorescence. However, at a higher DMSO fraction than 30%, the TTET efficiency was remarkably confined because of the increase of solvent viscosity. The decreased fluorescence quantum yields of the acceptors further reduced Φ_{UC} in the mixed solvents.

Surprisingly, when DPA was used as an acceptor, a larger molar fraction of DMSO led to weaker observed fluorescence. This behavior is completely different from that of the other acceptors. Recently, it has been confirmed that DPA can react with singlet oxygen to produce endoperoxides.[47] Thus, after irradiation for several seconds, the dissolved oxygen would be exhausted, and then the upconverted fluorescence intensity would decrease monotonically with the increasing fraction of DMSO, owing to reduced TTET efficiency and fluorescence quantum yield of the acceptor. A similar phenomenon was observed in the PtOEP/DPA system with air-saturated chloroform as solvent.[48] All observations show that a mixed solvent is feasible but inefficient for achieving TTA upconversion in aerated solutions.

Conclusions

Using different ligands, three Os(II) complexes were synthesized and applied as triplet photosensitizers in TTA upconversion. Owing to the heavy-atom effect, direct S–T transition of the photosensitizers was feasible. For Os-dipy, Os-phen, and Os-diphen, the lifetimes of the lowest triplet states were 107 ns, 373 ns, and 386 ns in deoxygenated dichloroethane, and the triplet energies determined from steady-state phosphorescence emission spectra were 1.75 eV, 1.80 eV, and 1.74 eV, respectively.

To reduce energy loss of TTET, DPA, perylene, and BPEA were chosen as the triplet acceptors as their triplet energies were relatively close. The strong upconverted fluorescence from these triplet acceptors was observed in the visible to violet range using the Os(II) complexes as photosensitizers. The upconverted fluorescence quantum yields were determined as 5.9%, 2.3%, and 12.5% for Os-phen/DPA, Os-phen/perylene, and Os-phen/BPEA, respectively, in deoxygenated dichloroethane. It is worth mentioning that an anti-Stokes shift of 1.14 eV was achieved from near-infrared to violet in the Os-phen/DPA system in solutions, which is the largest shift in all the reported experimental values to date. All the conclusions indicate that this system is a suitable candidate for solar energy applications.

The performances of these TTA upconversion systems were also assessed in aerated solutions. In a typical deoxygenating solvent, DMSO, Φ_{UC} values were significantly decreased because of the reduced TTET efficiency and fluorescence quantum yields, although quenching by oxygen was confined. For comparison, mixtures of dichloroethane and DMSO were also utilized as solvents for these TTA upconversion systems. It
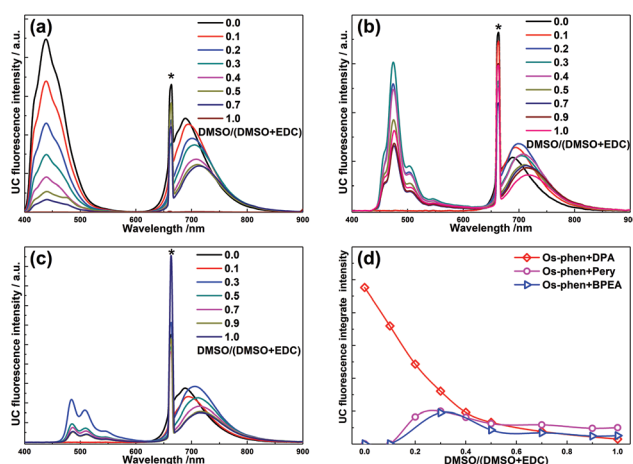
Fig. 6 TTA upconversion fluorescence spectra in air with Os-phen as photosensitizer (1 × 10⁻⁵ M). (a) c[DPA] = 5 × 10⁻³ M. (b) c[perylene] = 5 × 10⁻³ M, (c) c[BPEA] = 6.7 × 10⁻⁴ M. Mixed solvents of dichloroethane (EDC) and DMSO were used. (d) Upconverted fluorescence intensity *versus* the mole fraction of DMSO in the mixed solvents, as well as the photographs of upconverted fluorescence. λ_{ex} = 663 nm, P = 3800 mW cm⁻², 25 °C.

was found that the upconverted fluorescence intensities of the different acceptors exhibited different dependence on the DMSO fraction. The maximal TTA upconversion quantum yields were measured to be 4.5%, 0.8%, and 0.7% for Os-phen/DPA, Os-phen/perylene, and Os-phen/BPEA, respectively.

Thus, change of ligands in these Os(ɪɪ) complexes not only broadened the reported anti-Stokes shift, but also promoted the TTA upconversion quantum yield. The present work provides a synthetic tendency of Os(ɪɪ)-based triplet photosensitizers.

Experimental

DPA, perylene, BPEA, and methylene blue were purchased from Aladdin Reagent (Shanghai) Co., Ltd and used without any further purification. The synthetic procedure and structural characterization of the photosensitizers are described in the ESI.† Further details of the steady-state spectra, transient spectra, TTA upconversion spectra, and the corresponding kinetic measurements are also given in the ESI.†

Conflicts of interest

There are no conflicts to declare.

Acknowledgements

References

1 C. Ye, L. Zhou, X. Wang and Z. Liang, *Phys. Chem. Chem. Phys.*, 2016, **18**, 10818–10835.

2 A. Haefele, J. Blumhoff, R. S. Khnayzer and F. N. Castellano, *J. Phys. Chem. Lett.*, 2012, **3**, 299–303.

3 A. Monguzzi, R. Tubino, S. Hoseinkhani, M. Campione and F. Meinardi, *Phys. Chem. Chem. Phys.*, 2012, **14**, 4322–4332.

4 S. Baluschev, T. Miteva, V. Yakutkin, G. Nelles, A. Yasuda and G. Wegner, *Phys. Rev. Lett.*, 2006, **97**, 143903.

5 Y. Y. Cheng, B. Fückel, R. W. MacQueen, T. Khoury, R. G. Clady, T. F. Schulze, N. J. Ekins-Daukes, M. J. Crossley, B. Stannowski, K. Lips and T. W. Schmidt, *Energy Environ. Sci.*, 2012, **5**, 6953.

6 S. P. Hill and K. Hanson, *J. Am. Chem. Soc.*, 2017, **139**, 10988–10991.

7 B. Wang, B. Sun, X. Wang, C. Ye, P. Ding, Z. Liang, Z. Chen, X. Tao and L. Wu, *J. Phys. Chem. C*, 2014, **118**, 1417–1425.

8 A. Monguzzi, A. Oertel, D. Braga, A. Riedinger, D. K. Kim, P. N. Knüsel, A. Bianchi, M. Mauri, R. Simonutti and D. J. Norris, *ACS Appl. Mater. Interfaces*, 2017, **9**, 40180–40186.

9 H.-I. Kim, S. Weon, H. Kang, A. L. Hagstrom, O. S. Kwon, Y.-S. Lee, W. Choi and J.-H. Kim, *Environ. Sci. Technol.*, 2016, **50**, 11184–11192.

10 Q. Liu, T. Yang, W. Feng and F. Li, *J. Am. Chem. Soc.*, 2012, **134**, 5390–5397.

11 A. Nagai, J. B. Miller, P. Kos, S. Elkassih, H. Xiong and D. J. Siegwart, *ACS Biomater. Sci. Eng.*, 2016, **1**, 1206–1210.

12 J. Zhao, W. Wu, J. Sun and S. Guo, *Chem. Soc. Rev.*, 2013, **42**, 5323–5351.

13 N. Yanai and N. Kimizuka, *Acc. Chem. Res.*, 2017, **50**, 2487–2495.

14 J. Peng, X. Guo, X. Jiang, D. Zhao and Y. Ma, *Chem. Sci.*, 2016, **7**, 1233–1237.

15 H. Kouno, T. Ogawa, S. Amemori, P. Mahato, N. Yanai and N. Kimizuka, *Chem. Sci.*, 2016, **7**, 5224–5229.

16 S. Guo, L. Ma, J. Zhao, B. Küçüköz, A. Karatay, M. Hayvali, H. G. Yaglioglu and A. Elmali, *Chem. Sci.*, 2014, **5**, 489–500.

17 J. Wang, Y. Lu, W. McCarthy, R. Conway-Kenny, B. Twamley, J. Zhao and S. M. Draper, *Chem. Commun.*, 2018, **54**, 1073–1076.

18 Q. Zhou, M. Zhou, Y. Wei, X. Zhou, S. Liu, S. Zhang and B. Zhang, *Phys. Chem. Chem. Phys.*, 2017, **19**, 1516–1525.

19 T. N. Singhrachford and F. N. Castellano, *J. Phys. Chem. A*, 2009, **113**, 5912.

20 Y. Wei, M. Zheng, Q. Zhou, X. Zhou and S. Liu, *Org. Biomol. Chem.*, 2018, **16**, 5598–5608.

21 Y. Wei, M. Zhou, Q. Zhou, X. Zhou, S. Liu, S. Zhang and B. Zhang, *Phys. Chem. Chem. Phys.*, 2017, **19**, 22049–22060.

22 W. Wu, J. Zhao, J. Sun and S. Guo, *J. Org. Chem.*, 2012, **77**, 5305–5312.

23 K. Moor, J.-H. Kim, S. Snow and J.-H. Kim, *Chem. Commun.*, 2013, **49**, 10829.

24 R. Zhang, Y. Yang, S. Yang, V. S. P. K. Neti, H. Sepehrpour, P. J. Stang and K. Han, *J. Phys. Chem. C*, 2017, **121**, 14975–14980.

25 Z. Wang and J. Zhao, *Org. Lett.*, 2017, **19**, 4492–4495.

26 D. Wei, F. Ni, Z. Zhu, Y. Zou and C. Yang, *J. Mater. Chem. C*, 2017, **5**, 12674–12677.

27 J. Han, Y. Jiang, A. Obolda, P. Duan, F. Li and M. Liu, *J. Phys. Chem. Lett.*, 2017, **8**, 5865–5870.

28 D. Liu, Y. Zhao, Z. Wang, K. Xu and J. Zhao, *Dalton Trans.*, 2018, **47**, 8619–8628.

29 Y. Sasaki, S. Amemori, H. Kouno, N. Yanai and N. Kimizuka, *J. Mater. Chem. C*, 2017, **5**, 5063–5067.

30 S. Amemori, Y. Sasaki, N. Yanai and N. Kimizuka, *J. Am. Chem. Soc.*, 2016, **138**, 8702–8705.

31 H. Uoyama, K. Goushi, K. Shizu, H. Nomura and C. Adachi, *Nature*, 2012, **492**, 234–238.

32 W. L. Tsai, M. H. Huang, W. K. Lee, Y. J. Hsu, K. C. Pan, Y. H. Huang, H. C. Ting, M. Sarma, Y. Y. Ho, H. C. Hu,

C. C. Chen, M. T. Lee, K. T. Wong and C. C. Wu, *Chem. Commun.*, 2015, **51**, 13662–13665.

33 S. Altobello, R. Argazzi, S. Caramori, C. Contado, S. Da Fré, P. Rubino, C. Choné, G. Larramona and C. A. Bignozzi, *J. Am. Chem. Soc.*, 2005, **127**, 15342–15343.

34 T. Kinoshita, J.-I. Fujisawa, J. Nakazaki, S. Uchida, T. Kubo and H. Segawa, *J. Phys. Chem. Lett.*, 2012, **3**, 394–398.

35 V. Gray, D. Dzebo, M. Abrahamsson, B. Albinsson and K. Moth-Poulsen, *Phys. Chem. Chem. Phys.*, 2014, **16**, 10345–10352.

36 S. R. Johnson, T. D. Westmoreland, J. V. Caspar, K. R. Barqawi and T. J. Meyer, *Inorg. Chem.*, 1988, **27**, 3195–3200.

37 Y. T. Wang, X. Y. Liu, G. Cui, W. H. Fang and W. Thiel, *Angew. Chem., Int. Ed.*, 2016, **55**, 14009–14013.

38 A. Monguzzi, J. Mezyk, F. Scotognella, R. Tubino and F. Meinardi, *Phys. Rev. B: Condens. Matter Mater. Phys.*, 2008, **78**, 195112.

39 Y. Y. Cheng, B. Fuckel, T. Khoury, R. G. Clady, N. J. Ekins-Daukes, M. J. Crossley and T. W. Schmidt, *J. Phys. Chem. A*, 2011, **115**, 1047–1053.

40 F. Deng, J. Blumhoff and F. N. Castellano, *J. Phys. Chem. A*, 2013, **117**, 4412–4419.

41 C. Mongin, J. H. Golden and F. N. Castellano, *ACS Appl. Mater. Interfaces*, 2016, **8**, 24038–24048.

42 D. Dzebo, K. Moth-Poulsen and B. Albinsson, *Photochem. Photobiol. Sci.*, 2017, **16**, 1327–1334.

43 C. Ye, B. Wang, R. Hao, X. Wang, P. Ding, X. Tao, Z. Chen, Z. Liang and Y. Zhou, *J. Mater. Chem. C*, 2014, **2**, 8507–8514.

44 F. Marsico, A. Turshatov, R. Peköz, Y. Avlasevich, M. Wagner, K. Weber, D. Donadio, K. Landfester, S. Baluschev and F. R. Wurm, *J. Am. Chem. Soc.*, 2014, **136**, 11057–11064.

45 S. Wan and W. Lu, *Angew. Chem., Int. Ed.*, 2017, **56**, 1784–1788.

46 S. Wan, J. Lin, H. Su, J. Dai and W. Lu, *Chem. Commun.*, 2018, **54**, 3907–3910.

47 W. Fudickar and T. Linker, *Chem. – Eur. J.*, 2011, **17**, 13661–13664.

48 T. Ogawa, N. Yanai, A. Monguzzi and N. Kimizuka, *Sci. Rep.*, 2015, **5**, 10882.